

Published in final edited form as:

*Gastroenterology*. 2014 May ; 146(5): 1289–1300.e19. doi:10.1053/j.gastro.2014.01.056.

## Nanoparticles with Surface Antibody Against CD98 and Carrying CD98 Small Interfering RNA Reduce Colitis in Mice

Bo Xiao<sup>1,\*</sup>, Hamed Laroui<sup>1</sup>, Emilie Viennois<sup>1,4</sup>, Saravanan Ayyadurai<sup>1</sup>, Moiz A. Charania<sup>1</sup>, Yuchen Zhang<sup>1</sup>, Zhan Zhang<sup>2</sup>, Mark T. Baker<sup>1</sup>, Benyue Zhang<sup>2</sup>, Andrew T. Gewirtz<sup>2,3</sup>, and Didier Merlin<sup>1,4</sup>

<sup>1</sup>Center for Diagnostics and Therapeutics, Institute for Biomedical Science, Department of Biology and Department of Chemistry, Georgia State University, Atlanta, 30302, USA

<sup>2</sup>Center for Inflammation, Immunity and Infection, Department of Biology, Georgia State University, Atlanta, 30302, USA

<sup>3</sup>Department of Pathology, School of Medicine, Emory University, Atlanta, 30322, USA

<sup>4</sup>Atlanta Veterans Affairs Medical Center, Decatur, 30033, USA

### Abstract

**BACKGROUND & AIMS**—Nanoparticles have been explored as carriers of small interfering RNAs (siRNAs), and might developed to treat inflammatory bowel disease (IBD). Overexpression of CD98 on the surface of colonic epithelial cells and macrophages promotes development and progression of IBD. We developed an orally delivered hydrogel that releases nanoparticles with single-chain CD98 antibodies on their surface (scCD98-functionalized) and loaded with CD98 siRNA (siCD98). We tested the ability of the nanoparticles to reduce levels of CD98 in colons of mice with colitis.

**METHODS**—scCD98-functionalized siCD98-loaded nanoparticles were fabricated using a complex coacervation technique. We investigated the cellular uptake and lysosome escape profiles of the nanoparticles in Colon-26 cells and RAW 264.7 macrophages using fluorescence microscopy. Colitis was induced by transfer of CD4<sup>+</sup>CD45RB<sup>high</sup> T cells to Rag<sup>-/-</sup> mice or administration of dextran sodium sulfate to C57BL/6 mice. Mice were then given hydrogel (chitosan and alginate) containing scCD98-functionalized nanoparticles loaded with siCD98 or scrambled siRNA (control) via gavage.

© 2014 The American Gastroenterological Association. Published by Elsevier Inc. All rights reserved.

Corresponding author: Bo Xiao, Ph.D., Center for Diagnostics and Therapeutics, Institute for Biomedical Science, Department of Biology and Department of Chemistry, Georgia State University, Atlanta, 30302, USA, Telephone: +1 (404) 413 3597, Fax: +1 (404) 413 3580, bxiao@gsu.edu.

Disclosures: The authors have no potential conflicts to disclose.

Author contributions: B.X. designed, conducted and analyzed experiments; and wrote the manuscript. H.L. designed and analyzed experiments; and proof read the manuscript. E.V., S.A., M.A.C., Y.Z., Z.Z., M.B., B.Z. conducted experiments. A.T.G. edited the manuscript. D.M. designed experiments; supervised the project; and proof read the manuscript.

**Publisher's Disclaimer:** This is a PDF file of an unedited manuscript that has been accepted for publication. As a service to our customers we are providing this early version of the manuscript. The manuscript will undergo copyediting, typesetting, and review of the resulting proof before it is published in its final citable form. Please note that during the production process errors may be discovered which could affect the content, and all legal disclaimers that apply to the journal pertain.

**RESULTS**—The scCD98-functionalized nanoparticles were approximately 200 nm in size and had high affinity for CD98-overexpressing cells. The scCD98-functionalized siCD98-loaded nanoparticles significantly reduced levels of CD98 in Colon-26 cells and RAW 264.7 macrophages, along with production of inflammatory cytokines (TNF $\alpha$ , IL6, and IL12). In mice with colitis, administration of the scCD98-functionalized siCD98-loaded nanoparticles reduced colon expression of CD98. Importantly, the severity of colitis was also reduced, compared with controls (based on loss of body weight, myeloperoxidase activity, inflammatory cytokine production, and histologic analysis). Approximately 24.1% of colonic macrophages (CD11b<sup>+</sup>CD11c<sup>-</sup>F4/80<sup>+</sup>) in the mice had taken up fluorescently labeled siRNA-loaded nanoparticles within 12 hr of administration.

**CONCLUSIONS**—Nanoparticles containing surface CD98 antibody and loaded with siCD98 reduce expression of this protein by colonic epithelial cells and macrophages; oral administration decreases the severity of colitis in mice. This nanoparticle in hydrogel (chitosan/alginate) formulation might be developed to treat patients with IBD.

### Keywords

Mouse Model; CD98; Gene Silencing; Colitis-targeted Therapy

### Introduction

Inflammatory bowel disease (IBD), mainly including Crohn's disease and ulcerative colitis, is a chronic relapsing disorder of the gastrointestinal tract that can develop into colorectal cancer if inflammation is not adequately suppressed.<sup>1</sup> The main goals of IBD therapy are to induce and maintain clinical remission, achieve mucosal healing, and reduce surgeries and hospitalizations.<sup>2,3</sup> The modern approaches to develop IBD therapeutics can be divided into three categories: (1) the development of agents that inhibit the inflammatory cytokines (*e.g.*, anti-TNF $\alpha$ ) that induce the apoptosis of T-lymphocytes; (2) the identification of anti-inflammatory cytokines that down-regulate T-lymphocyte proliferation; and (3) the synthesis of selective adhesion molecule inhibitors that suppress the trafficking of T-lymphocytes into the gut epithelium.<sup>4</sup> The drugs capable of mediating these effects are usually administered at high doses and/or systemically, leading to significant adverse effects. Therefore, novel targeted delivery ligands and therapeutic targeting molecules are critically needed for IBD therapy. CD98 is a type II transmembrane protein in which a heavy chain (CD98hc or SLC3A2) and one of several versions of the L-type amino acid transporter 1 form a heterodimeric neutral amino acid transport system.<sup>5,6</sup> The cytoplasmic domains of CD98 can interact with  $\beta_1$  integrin to regulate integrin signaling-mediated functions, such as cell homeostasis, epithelial adhesion/polarity, and immune responses.<sup>6</sup> Previous studies have revealed that CD98 expression is highly up-regulated in colonic tissues from mice with active colitis,<sup>7</sup> colonic biopsies from patients with Crohn's disease,<sup>8</sup> and at the surface of intestinal B cells, CD4<sup>+</sup> T cells and CD8<sup>+</sup> T cells isolated from IBD patients.<sup>9</sup> Further study has shown that CD98 is highly expressed in intestinal macrophages and plays an important role in macrophage activation.<sup>10</sup> In addition, the loss of intestinal epithelial barrier and polarity functions induces the redistribution of basolateral proteins (*e.g.*, CD98) to apical cell surface during intestinal inflammation.<sup>11,12</sup> Our recent study

demonstrated that overexpression of CD98 in inflamed colon plays a vital role in the development and progression of IBD.<sup>1</sup> Thus, it is reasonable to speculate that a targeted therapeutic blockade of CD98 expression might offer an effective approach for IBD therapy.

Recently, RNA interference (RNAi) *via* the use of small interfering RNA (siRNA; 19–23 base pairs) has been developed as a powerful technology to silence disease-related genes. However, the therapeutic potential of siRNA has been extremely stymied by the absence of safe and efficient carriers for targeted delivery *in vivo*. siRNA has to cross organism, tissue and cell barriers to enter the cytoplasm, where it can guide the sequence-specific degradation of mRNA.<sup>13</sup> Chitosan is a biocompatible, biodegradable and cationic natural polymer that shows relatively high transfection efficiency and has been widely used for siRNA delivery.<sup>14</sup> Studies have shown that endosomal escape is the bottleneck for siRNA delivery, as above 90% of internalized nucleic acids are degraded in endosomes/lysosomes.<sup>15</sup> To avoid this degradation, proton buffering constituents, such as imidazole groups and polyethylenimine (PEI), can be used to disrupt endosomal/lysosomal membranes, thereby facilitating the escape of siRNA into the cytoplasm.<sup>16</sup> Mucus is another significant barrier that can impede localized drug delivery to the colonic mucosal surface *via* oral administration. To address this issue, NPs coated with high-density short poly(ethylene glycol) (PEG) molecules allow them to “slip” through mucus, showing a diffusion ratio greater than that of unmodified NPs.<sup>17</sup>

Here, we sought to develop a method for specific delivery of CD98 siRNA (siCD98) to inflamed colon following oral administration. To obtain efficient mucus transportation, targeted cellular uptake and endosomal/lysosomal escape of NPs, we fabricated single-chain CD98 antibody (scCD98)-PEG-urocanic acid-modified chitosan (scCD98-PEG-UAC)/PEI (2 kDa)/siCD98 NPs. To bypass the degradative effects of components in the gastrointestinal tract (*e.g.*, digestive acids and enzymes), we embedded our NPs in a hydrogel (chitosan/alginate) that selectively degraded in the vicinity of the inflamed colon. Our *in vitro* and *in vivo* results demonstrated that scCD98-functionalized siCD98-loaded NPs were efficiently taken up by CD98-overexpressing colonic cells, resulting in a decrease of the symptoms of IBD.

## Materials and Methods

See Supplementary Materials and Methods for additional information.

### Cell Culture

Colon-26 cells were maintained in RPMI 1640 medium containing L-glutamine, streptomycin, penicillin and fetal bovine serum (FBS). RAW 264.7 macrophages were cultured in Dulbecco's modified Eagle medium containing glucose, streptomycin, penicillin and FBS.

### Animals

Recombinase activating gene-1-deficient (RAG1<sup>-/-</sup>) mice (The Jackson Laboratory) and C57BL/6 mice (The Jackson Laboratory) were housed in respective germ-free facility and

clean facility. All the animal experiments were approved by Georgia State University Institutional Animal Care and Use Committee.

## Results

### Synthesis and Characterization of scCD98-PEG-UAC

We synthesized a novel polymer with proton buffering groups conjugated with scCD98. The synthetic scheme and physical characterization of scCD98-PEG-UAC are shown in Supplementary Figure 1–3. The degrees of amino-substitution of imidazole and PEG groups were estimated by  $^1\text{H}$  NMR as 28.3% and 4.9%, respectively. The generated polymer was used as a siRNA vector assisted by low-molecular-weight PEI (2 kDa).

### Fabrication and Characterization of scCD98-Functionalized NPs

As depicted in Supplementary Figure 4, the polymers and siRNA spontaneously formed condensed NPs and these NPs were equipped with targeting capacity by conjugating scCD98 to the surfaces; the antibody aimed to enhance the bind between scCD98-functionalized NPs and CD98 protein that is overexpressed on the surface of colonic epithelial cells and macrophages in IBD. A fundamental requirement for gene delivery is that vectors must be able to efficiently condense nucleic acids into NPs. Herein, the siRNA-condensation abilities of scCD98-PEG-UAC with or without PEI (2 kDa) were evaluated with an agarose gel retardation assay. As shown in Figure 1A, a substantial portion of siRNA was released from the NPs fabricated with scCD98-PEG-UAC and siRNA, and migrated into the gel, as demonstrated by a faint trace of signal even when the weight ratio reached 60:1. This suggested that the positive charges of scCD98-PEG-UAC might not be sufficient to form stable and condensed siRNA-loaded NPs. Given the high positive charge density of PEI and its wide application in gene delivery, we introduced PEI into our NPs and no obvious siRNA was released from NPs any more (Figure 1B). This might indicate that PEI could supply sufficient positive charges to interact with the negative-charged siRNA. Additionally, they could also induce chain entanglement effects with scCD98-PEG-UAC and siRNA, resulting in the formation of condensed NPs. The results of dynamic light scattering indicated that NPs were 1473261 nm in size, and their zeta potentials were in the range of 7.9317.3 mV (Figure 1C and 1D). Atomic force microscopy further comparatively confirmed the size of the spherical NPs (Figure 1E and Figure 1F). It was proposed that most cells can efficiently internalize slightly positive-charged particles with a size less than several hundred nanometers.<sup>18, 19</sup> So the NPs above are thought to be favorable to deliver siRNA into cells.

### Surface Plasmon Resonance (SPR) Assays of NPs to CD98 Protein

To investigate whether scCD98 presented on the surface of NPs were available for specific binding, we performed SPR. Successive injections of CD98 or bovine serum albumin (BSA, negative control) solutions ensured sufficient proteins coated on the SPR chips, demonstrated by the deflection of resonance angle. As seen in Supplementary Figure 5, linkage of CD98 resulted in SPR resonance angle changes of 52 mDeg, equivalent to 520 pg/mm<sup>2</sup> of immobilized protein. As expected, there were significant differences in the binding of NPs with or without scCD98 to the CD98 protein-coated chip. A dramatic

increase (~3.8-fold) in the degree of resonance angle change was observed for scCD98-functionalized NPs compared to non-functionalized NPs. In contrast, slight binding was observed between scCD98-functionalized NPs and BSA (negative control) (Supplementary Figure 6). Taken together, these results strongly implicated that scCD98-functionalized NPs should preferentially bind to CD98-overexpressing cells compared to non-functionalized NPs.

### **NPs Do Not Affect Cell Viability**

Cytotoxicity is a primary concern in the development of gene vehicles. To evaluate the cytotoxicity of our NPs, we treated Colon-26 and RAW 264.7 cells with scCD98-functionalized NPs (siRNA, 100 nM) for 6 h and tested cell viability using 3-(4,5-dimethylthiazol-2-yl)-2,5-diphenyl tetrazolium bromide (MTT) assays. We did not observe any alteration of the cell viability in response to our NPs (Figure 2A). However, it should be noted that PEI (2 kDa)/siRNA complexes (weight ratio, 40:1) exhibited significant toxicity compared to scCD98-functionalized NPs (weight ratio, 40:40:1). It is well known that excess positive charges on the NP surface can interact with cellular components and impair membrane integration.<sup>20, 21</sup> Meanwhile, cationic polymers may also interfere with critical intracellular processes, disrupting protein kinase C function, and eventually eliciting cell death.<sup>22</sup> Thus, it was speculated that the scCD98 and PEG groups of scCD98-PEG-UAC were exposed at the surfaces of the NPs, subsequently decreasing the interactions between NPs and the negatively charged constituents of the cells. This allowed our NPs to exhibit much better biocompatibility than PEI (2 kDa)/siRNA complexes. Oligofectamine and branched PEI (bPEI, 25 kDa), which are the most frequently used gene carriers, were used as controls. Oligofectamine/siRNA complexes applied at the recommended transfection condition showed significantly higher cytotoxicity compared to our scCD98-functionalized NPs, and bPEI (25 kDa)/siRNA (weight ratio, 40:1) complexes inhibited the proliferation of both cell lines by over 66.2%. This might explained why Oligofectamine and bPEI (25 kDa) were recommended for transfection of highly confluent cells, enabling the survival of sufficient cells for subsequent experiments.

MTT assay is not suitable for real-time analysis of NP cytotoxicity, so we also used electrical impedance sensing (ECIS) for *in vitro* toxicity tests. Initially, Caco2-BBE cells attached to the electrode surface to form a confluent layer with a resistance of around 40,000 Ohms (Figure 2B). Such cell layers were then co-incubated with different NPs (siRNA, 100 nM). After 20 h of co-incubation, scCD98-functionalized NPs-treated Caco2-BBE monolayers yielded a slight increase in resistance. Conversely, the cell monolayer co-incubated with bPEI (25 kDa)/siRNA complexes (40:1) experience sharp decrease in resistance. These results indicated that scCD98-functionalized NPs did not show obvious cytotoxicity or deleterious effects on monolayer resistance (representing intestinal barrier function).

### **NPs are Internalized by Epithelial Cells, Macrophages, BMDMs and Colitis Tissue**

Efficient cellular uptake and endosomal escape are major requirements for the therapeutic use of siRNA. As seen in Figure 3A, numerous scCD98-functionalized fluorescein isothiocyanate (FITC)-siRNA-loaded NPs (weight ratio, 40:20:1) were taken up by most

Colon-26 and RAW 264.7 cells after 6 h of exposure. Imaging of individual cells also revealed that NPs appeared to localize at the perinuclear region rather than in the nucleus. Moreover, scCD98-functionalized NPs yielded much stronger fluorescence intensities compared to Oligofectamine/FITC-siRNA complexes (Supplementary Figure 7). As previously reported, the continuous subculture of immortalized macrophage-like myeloid cells (*e.g.*, RAW 264.7 macrophages) under selective pressure induces a loss of genes that are important for macrophage function.<sup>23</sup> We thus tested the cellular uptake of scCD98-functionalized NPs in bone marrow-derived macrophages (BMDMs), which are primary macrophages that have been widely used because of their homogeneity, proliferation capacity, long lifespan, and ease of harvesting.<sup>24, 25</sup> As shown in Supplementary Figure 8, an assessment of cellular uptake at different time points (0, 1, 3, and 6 h) revealed a time-dependent increase in the FITC fluorescence signals of NPs in BMDMs. After 6 h, green fluorescence was mainly detected in the cytoplasm of almost all cells.

To investigate whether the introduction of pH-buffering moieties could induce efficient endosomal escape, we stained the endolysosomal compartments of transfected Colon-26 and RAW 264.7 cells with LysoTracker<sup>®</sup> Red (Supplementary Figure 9). After 6 h of co-incubation, NPs (green) were internalized to the interiors of cells, where some of them overlapped with the lysosome signals to produce yellow spots. Meanwhile, partial of NPs did not perfectly overlap with endosome/lysosome (red), indicating that the NPs were released from the endolysosomal compartment. The above experiments demonstrated that our NPs can be efficiently internalized into cells, and further exhibit excellent lysosomal escape ability.

We next evaluated the tissue biodistribution of scCD98-functionalized NPs based on *ex vivo* experiment. Tissue cross-sections showed that large amount of NPs (green) accumulated in colonic epithelial cells after 6 h of co-incubation with colitis tissue (Figure 3B). Interestingly, we also found that amounts of NPs penetrated deep into the mucosa and were taken up by the cells (*e.g.*, macrophages).

We further quantitatively compared the cellular uptake of different NPs in Colon-26 and RAW 264.7 cells using FCM. As shown in Figure 4A and 4C, Colon-26 cells co-incubated with scCD98-functionalized NPs exhibited much stronger fluorescence intensity at each time point (1.7- and 1.3-fold at 3 and 6 h, respectively) than those co-incubated with non-functionalized NPs, indicating that scCD98 functionalization significantly increased the cellular uptake of NPs through active targeting. In addition, no differences in cellular uptake for scCD98-functionalized NPs were apparent at 3 and 6 h, indicating that scCD98-functionalized NPs were internalized much more rapidly by cells than non-functionalized NPs. RAW 264.7 cells exhibited similar NP-uptake profiles as Colon-26 cells (Figure 4B and 4D).

To further demonstrate the targeting effect of scCD98 functionalization, we depleted CD98 in Colon-26 and RAW 264.7 cells using RNAi technology (Supplementary Figure 10A) and then tested the transfection efficiency of scCD98-functionalized NPs. We observed approximately a 42.8% and 59.8% reduction of NP uptake in Colon-26 and RAW 264.7 cells, respectively, upon knockdown of CD98, confirming the targeting role of scCD98 on

the surface of NPs (Supplementary Figure 10B–D). The further decrease in the cellular uptake efficiency of scCD98-functionalized NPs in transfected cells compared with that of non-functionalized NPs indicates that CD98 plays an important role in cellular activity.

### CD98 is Down-regulated by scCD98-Functionalized NPs *In Vitro*

We next sought to assess whether scCD98-functionalized NPs could be used to knockdown the expression of CD98 in Colon-26, RAW 264.7 and BMDMs using qRT-PCR. Relative to untreated Colon-26 cells and cells treated with scrambled siRNA-loaded NPs, scCD98-functionalized siCD98-loaded NPs produced marked decrease of CD98 (Figure 5A and Supplementary Figure 11A). NPs (weight ratio, 40:20:1) exhibited comparatively gene knockdown efficiency (~84.5%) compared with Oligofectamine/siRNA complexes (~73.6%), indicating that our NPs had an efficient CD98 down-regulation effect on Colon-26 cells. As shown in Figure 5B, compared to cells treated with lipopolysaccharide (LPS, 5 µg/mL), significantly lower CD98 mRNA expression levels in all the NP-treated cells were observed. A particularly large decrease was seen in response to scCD98-functionalized NPs (weight ratio, 40:20:1), which decreased the expression of CD98 to 27% of the control level. This decrease in gene expression was statistically significant compared to Oligofectamine, which decreased CD98 expression to 36%. Notably, the concentration of siCD98 contained in scCD98-functionalized NPs was around half of that used in Oligofectamine/siRNA experiments. With silencing efficiency very similar to Oligofectamine, scCD98-functionalized NPs (weight ratio, 40:20:1) were deemed suitable for the *in vivo* experiments.

We next questioned whether the NP-mediated down-regulation of CD98 could attenuate inflammation *in vitro*. Most strikingly, we found that the significant decrease in CD98 mRNA levels attenuated the activation of pro-inflammatory cytokines in IBD, namely TNF $\alpha$ , IL6 and IL12 (Figure 5C–E). Appropriate controls were also performed here, and the results showed that scCD98-functionalized scrambled siRNA-loaded NPs did not produce obvious knockdown of CD98 and pro-inflammatory cytokines relative to LPS-stimulated macrophages (Supplementary Figure 11B). These results suggested that CD98 might be a critical factor in IBD, and that decreasing its expression could potentially alleviate IBD-related inflammation. Moreover, scCD98-functionalized siCD98-loaded NPs induced the same trend toward decreased CD98, TNF $\alpha$ , IL6 and IL12 in BMDMs as they did in RAW 264.7 macrophages (Supplementary Figure 12). Finally, we also tested the stability of our NPs with respect to RNAi efficiency *in vitro*. It was found that RNAi efficiency decreased over time (Supplementary Figure 13), indicating that it is best to use freshly prepared NPs.

### Hierarchical NPs in Hydrogels Reduce Chronic Colitis

A T-cell transfer mouse model of chronic colitis is the prototypical and best-characterized model of chronic colitis.<sup>26</sup> It is recognized to be more relevant to human IBD (especially Crohn's disease) compared with traditional acute colitis.<sup>27</sup> Here, we examined the anti-inflammatory effect of scCD98-functionalized siCD98-loaded NPs (weight ratio, 40:20:1) in this mice model. As shown in Figure 6A, injection of RAG<sup>-/-</sup> mice with FCM-purified CD4<sup>+</sup> CD45RB<sup>high</sup> T cells (Supplementary Figure 14) resulted in a characteristic loss of body weight that started 3 week after injection, a result that is in agreement with a previous

report.<sup>26</sup> However, oral administration of hydrogel containing scCD98-functionalized siCD98-loaded NPs (treatment group) significantly reduced weight loss at week 9 compared with untreated mice or mice treated with hydrogel containing scCD98-functionalized scrambled siRNA-loaded NPs (treatment control group). Colonic myeloperoxidase (MPO) activity was measured to provide an indication of the extent of neutrophil infiltration. As shown in Figure 6B, MPO levels in the colon were clearly increased in mice that received a T-cell transfer. Treatment group showed markedly reduced MPO (~65.7%) compared with untreated group. We further tested the mRNA expression levels of CD98 and pro-inflammatory cytokines (Figure 6C). CD98 mRNA expression in treatment group was decreased by approximately 65.0% compared to untreated group. Interestingly, the mRNA expression of TNF $\alpha$ , IL6 and IL12 were also decreased (59.9%, 80.4%, and 31.8%, respectively). Overall, the levels of CD98 and pro-inflammatory cytokines were much lower in the treatment group compared with untreated mice or treatment control group. The anti-inflammatory effect of scCD98-functionalized siCD98-loaded NPs was confirmed at the histologic level using H&E-stained colonic sections (Figure 6D). The negative control mice showed an intact epithelium, normal numbers of goblet cells, and a lack of inflammatory cell infiltration. In contrast, adoptive transfer of T cells into RAG<sup>-/-</sup> mice induced obvious chronic colitis—characterized by a loss of goblet cells, extensive mucosal and transmural injury, and infiltration of immune cells—affecting all layers of the colon. However, mice in the treatment group showed markedly reduced intestinal inflammation.

### Hierarchical Nanoparticle in Hydrogel Reduce DSS-Induced Acute Colitis

The DSS-induced acute colitis mouse model is an easy induced and highly reproducible model that can be correlated with human IBD, especially ulcerative colitis.<sup>27, 28</sup> Here, we also investigated whether orally delivered scCD98-functionalized siCD98-loaded NPs (weight ratio, 40:20:1) could mitigate the clinical manifestation of DSS-induced acute colitis in a mouse model. Body weight changes among DSS-treated mice were evaluated after administration of hydrogel with or without NPs. As seen in Figure 7A, after 6 days, mice in the DSS control group (DSS + hydrogel without NPs) had a body weight loss of  $18.1 \pm 1.24\%$ , which was about twice as much as that of mice in the treatment group (DSS + hydrogel with scCD98-functionalized siCD98-loaded NPs;  $8.7 \pm 0.75\%$ ). These decreases in body weight were correlated with substantial increases in MPO activity and the expression levels of CD98 and pro-inflammatory factors. As shown in Figure 7B, colonic MPO activity in the treatment group was significantly lower than that in the DSS control group. In the case of mRNA expression levels, we observed a 47.7% decrease of CD98 expression in the treatment group compared to the DSS control group (Figure 7C). This was accompanied by marked knockdown of TNF $\alpha$ , IL6 and IL12 (26.0%, 81.2% and 71.2%, respectively). Overall, the levels of CD98 and pro-inflammatory cytokines were much lower in the treatment group compared to the DSS control group. H&E-stained colon cryosections were evaluated for histological changes (Figure 7D). The negative control group (H<sub>2</sub>O + hydrogel without NPs) had normal colon histology, with no sign of inflammation or disruption of healthy tissue morphology. Colon tissues from the DSS control group or treatment control group (DSS + hydrogel with scCD98-functionalized scrambled siRNA-loaded NPs) exhibited clear signs of inflammation, including epithelial disruption, goblet cell depletion,



and significant infiltration of inflammatory cells into the mucosa. In contrast, tissues from the treatment group showed much less inflammation.

To examine whether scCD98-functionalized NPs could target colonic epithelial cells and macrophages *in vivo*, we gavaged DSS-treated mice with hydrogel containing scCD98-functionalized FITC-siRNA-loaded NPs and carried out FCM. As shown in Figure 7E–F, approximately 24.1% of the tested colonic macrophages (CD11b<sup>+</sup>CD11c<sup>-</sup>F4/80<sup>+</sup>) had taken up NPs by 12 h post-administration, and ~9.6% of colonic epithelial cells exhibited FITC signals. A previous study demonstrated that NP formulations with cellular uptake rates of ~5% to 20% following a single oral administration could show effective function *in vivo*.<sup>29</sup> Our results are in good agreement with this finding. In addition, we found that mice in the treatment group had significantly fewer CD98-positive epithelial cells and macrophages compared to DSS control group and treatment control group (Supplementary Figure 15A). Furthermore, we also found that cellular uptake of scCD98-functionalized NPs decreased in the treatment group in comparison to DSS control group after 5 days of DSS treatment, even though there is no statistically significant difference between these two groups (Supplementary Figure 15B). Taken together, our *in vivo* results indicate that NPs-embedded hydrogel can induce efficient colitis tissue-targeted delivery of siCD98 to epithelial cells and macrophages, and thus could significantly contribute to future developments in IBD therapy.

## Discussion

This report underscores the substantial NPs targeted delivery ligand and therapeutic targeting molecule of CD98 in IBD therapy. We designed an antibody-functionalized NP-releasing hydrogel to specifically target CD98-overexpressing cells, thereby facilitating the delivery of therapeutic siCD98 to the inflamed colon. Our experiments demonstrated that scCD98-functionalized siCD98-loaded NPs could down-regulate CD98 and efficiently attenuate the manifestations of IBD *in vitro*, and in both T-cell transfer chronic colitis mouse model and DSS-induced acute colitis mouse model.

CD98 has been recognized as an important membrane protein in viral infection, inflammation disease and various cancers.<sup>1, 30, 31</sup> In colon tissues, the specific molecular ratio between CD98/LAT1 and  $\beta_1$  integrin might determine the polarity of epithelial cells.<sup>5</sup> However, CD98 is significantly up-regulated in both epithelial cells and immune cells during inflammation.<sup>7, 32</sup> The overexpression of CD98 in intestinal epithelial cells changes the ratio of CD98/LAT1 and  $\beta_1$  integrin, triggering a loss of epithelial cell polarity, which is a characteristic feature of IBD.<sup>7</sup> We previously produced intestinal epithelial cell CD98-overexpressing mice and CD98-knockdown mice. Surprisingly, we found that overexpression of CD98 stimulated cell proliferation and the production of pro-inflammatory mediators, whereas CD98-knockdown mice attenuated the inflammatory response and conferred resistance to DSS-induced colitis.<sup>1</sup> Thus, we speculated that CD98 could act as both NPs targeted delivery ligand and therapeutic targeting molecule for IBD treatment. Here, we hypothesized that NP-mediated CD98 knockdown could mitigate colitis in a mouse model. Accordingly, we designed a siCD98-loaded NP-releasing hydrogel to overcome the organism, tissue and cell barriers. Previous work has shown that the conjugation of antibodies to the surface of NPs could facilitate their internalization by the

desired cells, thus improving therapeutic efficacy.<sup>33</sup> Our comparative cellular uptake experiments indicated that scCD98-functionalized NPs were taken up into cells more readily than non-functionalized NPs. Furthermore, the siRNA-loaded NPs were efficiently released to the cytoplasm based on the results of lysosome escape experiments, suggesting that the imidazole groups and PEI (2 kDa) in the NPs functioned as efficient “proton-sponge” molecules in our system.

In macrophages treated with LPS *in vitro*, up-regulation of CD98 expression was correlated with increasing in the expression levels of the pro-inflammatory cytokines (TNF $\alpha$ , IL6 and IL12). Our laboratory previously optimized the formulation of NPs so that they can be administered *via* the oral route and break down at a pH similar to that found in the colon.<sup>34–36</sup> When mice with chronic colitis or acute colitis were dosed with scCD98-functionalized siCD98-loaded NP-releasing hydrogel, colitis symptoms were significantly attenuated. This suggested that both chronic colitis and acute colitis were ameliorated by knockdown of CD98 in colon tissues. In addition, FCM showed that our antibody-functionalized NPs can be preferentially taken up by colonic epithelial cells and macrophages. Together, our *in vitro* and *in vivo* data suggest that local targeting of CD98 expression can help ameliorate the symptoms of intestinal inflammation. Future studies are needed to determine whether this strategy could achieve healing in IBD patients.

Overall, we believe that this study represents an important new step toward the application of CD98 as a NP targeted delivery ligand and therapeutic targeting molecule in IBD therapy. Furthermore, our orally administered scCD98-functionalized NP-based method for the site-specific delivery of siCD98 should have fewer side effects than systemic delivery systems, and could help translate RNAi-based therapies from basic science to clinical application in IBD.

## Supplementary Materials and Methods

### Preparation and Characterization of scCD98-PEG-UAC

The synthetic strategy of scCD98-PEG-UAC is outlined in Supplementary Figure 1. Chitosan (Sigma) was obtained by further deacetylating and depolymerizing commercial chitosan using alkali treatment and sodium nitrite, respectively. Degree of deacetylation of chitosan was estimated as 95.6% by <sup>1</sup>H NMR. Molecular weight of the resultant chitosan was measured as 11.4 kDa by MOLDI-TOF. The UAC sample was synthesized described in previous report [1]. UAC-PEG-MAL was prepared in phosphate-buffer solution (PBS, pH = 7.2) through specific reaction between UAC and the NHS groups of bifunctional PEG derivative (NHS-PEG-MAL, MW 2000, Jenkem, Beijing, China) at the mole ratio of 1:4 overnight while stirring. The resulting conjugate was purified by ultrafiltration with an Amicon<sup>®</sup> Ultra (regenerated cellulose membrane, MWCO = 10 kDa, Millipore). Meanwhile, CD98 antibody (Biologend) was reduced to single-chain CD98 antibody (scCD98) using 2-mercapto ethylamine (Sigma). Then MAL-PEG-UAC was reacted with scCD98 at mole ratio of 1:2 in PBS (pH = 7.2) for 24 h at room temperature. The terminal MAL groups of MAL-PEG-UAC were specifically reacted with the thiol groups of scCD98, resulting in scCD98-PEG-UAC. Unreacted maleimide groups were quenched with 5 eq.

cysteine. The final conjugates were lyophilized and characterized by FT-IR and  $^1\text{H}$  NMR. SDS-PAGE was used to demonstrate the full reaction of thiolated scCD98.

Infrared spectra of chitosan and its derivatives were recorded with a Varian 600-UMA FT-IR microscope equipped with a liquid  $\text{N}_2$  cooled HgCdTe detector and coupled to a Varian 7000 FT-IR spectrometer. NMR spectrum was recorded on a Bruker Avance spectrometer (INOVA-600 NMR). 20 mg of samples were dissolved in  $\text{D}_2\text{O}$  to prepare a 2 wt % solution for  $^1\text{H}$  NMR measurement.

### **Fabrication of scCD98-Functionalized NPs**

scCD98-PEG-UAC and PEI (2 kDa) were dissolved in RNase-free water (4 mg/mL) and filtered by 0.22  $\mu\text{m}$  filters, respectively. The scrambled siRNA, FITC-siRNA or siCD98 stock solution was prepared in RNase-free water with the concentration of 0.1 mg/mL. NPs were prepared by a complex coacervation technique. Equivalent volumes of siRNA solutions were added to appropriate amount of sample solutions at various weight ratios and vortexed for 10 s. The resulting complexes were allowed to incubate for 30 min at room temperature for complete NP formation. NPs were prepared immediately prior to the experiments.

### **Protection of siRNA by NPs**

The siRNA binding capacities of NPs formed by scCD98-PEG-UAC and scrambled siRNA with or without PEI (2 k) were evaluated by agarose gel electrophoresis. 10  $\mu\text{L}$  of different complexes suspensions with various weight ratios were loaded into individual wells of agarose gel, and the electrophoresis was conducted on a 4% agarose gel at 100 V for 25 min in  $1\times\text{TAE}$  buffer. The resulting siRNA migration patterns were viewed under UV transilluminator. GelRed (Biotium, Hayward, CA) was used to stain siRNA.

### **Particle size, Zeta potential and Topographical Morphology Measurements**

Particle sizes (nm) and zeta potential (mV) of nanoparticles (NPs) were measured by dynamic light scattering using 90 Plus/BI-MAS (Multi angle particle sizing) or dynamic light scattering after applying an electric field using a ZetaPlus (Zeta potential analyzer, Brookhaven Instruments Corporation). The average and standard deviations of the diameters (nm) or zeta potential (mV) were calculated using 3 runs. Each run is an average of 10 measurements. For atomic force microscopy test, a drop of scCD98-functionalized NPs (weight ratio, 40:20:1) suspension was deposited onto a freshly cleaved mica slide, followed by drying overnight at 25  $^\circ\text{C}$ . The images were taken using a SPA 400 AFM (Seiko instruments Inc., Chiba, Japan) at tapping mode using high resonant frequency ( $F_0 = 150$  kHz) pyramidal cantilevers with silicon probes at a scan frequency of 1 Hz.

### **Binding Affinity Measurement by Surface Plasmon Resonance (SPR)**

The interaction between scCD98-functionalized NPs or non-functionalized NPs and CD98 protein (Sino Biological Inc., Beijing, China) or BSA were investigated using the BI-2000 Biosensing Instrument (Tempe, AZ), based on the SPR theory. Briefly, after coating the chip with CD98 protein or BSA, NPs suspensions with the same concentration and volume were passed on. As a result, a two-step interaction curve was obtained. The first step involved

adsorption of NPs on CD98 or BSA until maximum NPs adsorption was represented. In the second step, when the passing NPs concentration reached null concentration, the running buffer released “unspecific” adsorption. The kinetics of the adsorption curve decreased to a plateau at an intermediate level above the initial baseline. The amplitude of NPs binding to CD98 or BSA represents the difference between the initial and final levels.

### **Biocompatibility of NPs**

For MTT assay (Invitrogen, Eugene, OR), Colon-26 cells and RAW 264.7 macrophages were seeded at a respective density of  $2 \times 10^4$  and  $8 \times 10^3$  cells/well in 96-well plates and incubated overnight. The cells were incubated with freshly prepared NPs suspensions for 6 h, and the scrambled siRNA concentration in the medium is set as 100 nM. Cells were then incubated with MTT (0.5 mg/mL in supplemented 100  $\mu$ L of serum-free DMEM) at 37 °C for 4 h. Thereafter, the media were discarded and 50  $\mu$ L DMSO was added to each well prior to spectrophotometric measurements at 490 nm. Untreated cells were used as a negative reference, whereas bPEI (25 kDa)/siRNA complexes (weight ratio, 40:1) and Oligofectamine/siRNA complexes, the most frequently used gene carriers, were selected as positive references.

Cell-attachment assays were performed to investigate the real-time cytotoxicity of NPs using ECIS technology (Applied BioPhysics). The ECIS model 1600R was used for these experiments. The measurement system consists of an 8-well culture dish (ECIS 8W1E plate), the surface of which is seeded with Caco2-BBE cells at a density of  $1 \times 10^6$  cells/well. Once cells reached confluence, NPs were added to the wells and the siRNA concentration in the medium is set as 100 nM. Control cell culture was used for each experiment, and the toxicity of bPEI (25 kDa)/siRNA complexes (weight ratio, 40:1) was also tested. Basal resistance measurements were performed using the ideal frequency for Caco2-BBE cells, 500 Hz, and a voltage of 1 V.

### **Differentiation of BMDMs**

Bone marrow was harvested from the femurs of C57BL/6 mice (12-wk-old). Red blood cells were lysed using ammonium chloride and EDTA. To obtain BMDMs, cells were cultured in RPMI 1640 medium supplemented with 10% fetal bovine serum (Atlanta Biologicals) and 8% L929-cell conditioned medium (as a source for macrophages colony stimulating factor). Cells were maintained at 37°C in 5% CO<sub>2</sub>-humidified atmosphere for 5 days to get BMDMs.

### ***In Vitro* Cellular Uptake and Lysosomal Escape of scCD98-Functionalized NPs**

Colon-26 cells and RAW 264.7 macrophages were seeded in eight-chamber tissue culture glass slide (BD Falcon) at a respective density of  $4.0 \times 10^4$  and  $3 \times 10^3$  cells/well and incubated overnight. The culture medium was exchanged to serum-free medium containing scCD98-functionalized FITC-siRNA (Life Technologies)-loaded NPs (weight ratio, 40:20:1). The FITC-siRNA concentration in the medium is set as 100 nM. After 6 h of incubation, the cells (Colon-26 cells and RAW 264.7 macrophages) were thoroughly rinsed with cold PBS to eliminate excess of NPs, and then fixed in 4% paraformaldehyde for 20 min. To observe cellular uptake of NPs, DAPI (Invitrogen) was diluted 10,000 times and

added for staining nucleus for 5 min. BMDMs was tested for cellular uptake at different time points (0, 1, 3 and 6 h), and Oligofectamine reagent (Invitrogen) was used as control siRNA carrier. To observe lysosomal escape of NPs, cells were subsequently stained with 50 nM LysoTracker Red (Invitrogen) for 30 min and DAPI for 5 min. Images were acquired using an Olympus equipped with a Hamamatsu Digital Camera ORCA-03G.

### **Ex Vivo Cellular Uptake of Nanoparticles**

Colitis was induced in male C57BL/6 mouse (10–12-wk-old) by replacing their drinking water with a 3.5% (wt/vol) DSS (36–50 kDa). After six days of DSS treatment, mice were sacrificed and colon was removed for further study. Colitis tissues (6–8 mm) were placed in 24-well culture plates with the mucosal surface facing upwards. The wells were flooded in serum-free RPMI-1640 medium supplemented with penicillin and streptomycin, and then scCD98-functionalized FITC-siRNA-loaded NPs (weight ratio, 40:20:1) were added. The final FITC-siRNA concentration in the medium is set as 200 nM. After 6 h, tissues were rinsed thoroughly 3 times with cold PBS and embedded in OCT. sections (6  $\mu$ m) were stained with Alexa Fluor 568 phalloidin and DAPI. Images were acquired using an Olympus equipped with a Hamamatsu Digital Camera ORCA-03G.

### **Quantification of Cellular Uptake of NPs**

Colon-26 cells and RAW 264.7 macrophages were seeded in 12-well plates at  $2 \times 10^5$  and  $1 \times 10^5$  cells/well, respectively, and incubated overnight. The culture medium was replaced with serum-free medium containing scCD98-functionalized NPs or non-functionalized NPs (weight ratio, 40:20:1). The final FITC-siRNA in the medium was 100 nM. Untreated cells were used as a negative control. After incubating for 3 and 6 h, the cells were thoroughly rinsed with cold PBS to eliminate excess NPs that had not been taken up by the cells. Subsequently, treated cells were harvested using accutase or trypsin, transferred to centrifuge tubes, and centrifuged at 500 g for 3 min. Upon removal of the supernatant, the cells were re-suspended in 0.5 mL of FCM buffer, transferred to 5 mL round-bottom polystyrene test tubes (BD Falcon), and kept at 4 °C until analysis. Analytical FCM was performed using the FITC channel on a FCM Canto system (BD Biosciences). A total of 10,000 ungated cells were analyzed.

The cellular targeting specificity of NPs was evaluated in Colon-26 cells and RAW 264.7 macrophages in which CD98 expression levels had been down-regulated by siRNA using Oligofectamine/siCD98 (Santa Cruz Biotechnology) complexes. Oligofectamine reagent was used according to the manufacturer's instructions. After co-incubation for 6 h, the cellular uptake of NPs by CD98-knockdown Colon-26 cells and RAW 264.7 macrophages was further investigated using FCM.

### **In Vitro Gene Silencing Efficiency Test**

Colon-26 and RAW 264.7 macrophages were seeded in 6-well plates at a respective density of  $3 \times 10^5$  and  $1 \times 10^5$  cells/well and incubated overnight. ScCD98-functionalized siCD98-loaded NPs were added for 6 h. The siRNA concentration in the medium is set as 100 nM. BMDMs were also investigated in RNAi test following the protocols as RAW 264.7 cells. As controls, cells were transfected with scrambled siRNA-loaded NPs and Oligofectamine/

siCD98 complexes. To investigate their half-life, NPs fabricated 1, 3, 5 and 7 days before the tests were also tested here. After co-culture, cells were incubated in DMEM medium containing 10% FBS for 18 h. Cells were then stimulated with lipopolysaccharide (LPS, 5 µg/mL, Sigma) for 3 h. Total RNA was extracted using RNeasy Plus Mini Kit (Qiagen). The cDNA was generated from the total RNAs isolated above using the Maxima first strand cDNA synthesis kit (Fermentas) according to the manufacturer's instruction. Levels of CD98 RNA expression were quantified by RT-PCR using Maxima® SYBR Green/ROX qPCR Master Mix (Fermentas). The data were normalized to the internal control: 36B4. Relative gene expression levels were calculated using the delta delta Ct ( $2^{-\Delta\Delta C_t}$ ) method. Sequences of all the primers used for RT-PCR are given in Supplementary Table 1.

### Induction of Chronic Colitis and Oral siRNA Delivery

Chronic colitis was induced by the transfer of sorted wild-type CD4<sup>+</sup>CD45RB<sup>high</sup> T cells into RAG1<sup>-/-</sup> mice (8-wk-old) according to a published method.<sup>[2, 3]</sup> Briefly, spleens were removed from donor C57BL/6 mice (11-wk-old) and teased into a single-cell suspension in PBS/4% fetal bovine serum solution. CD4<sup>+</sup> cells were positively selected using a MACS CD4<sup>+</sup> isolation kit (Miltenyi Biotec). Enriched CD4<sup>+</sup> T cells were labeled with APC-conjugated anti-mouse CD4 and PE-conjugated anti-mouse CD45RB antibody (eBioscience), and sorted into a CD45RB<sup>high</sup> (45% brightest) fraction using FACSARIA (BD Biosciences). A post-sort analysis showed that these cells were > 99% pure. Male RAG1<sup>-/-</sup> mice were intravenously injected with  $1 \times 10^6$  CD4<sup>+</sup>CD45RB<sup>high</sup> T cells per mouse. scCD98-functionalized NPs (weight ratio, 40:20:1) were specifically delivered into the colonic lumen of mice by encapsulating them in a hydrogel composed of alginate and chitosan at a ratio of 7/3 (wt/wt). A detailed protocol is available at [http://www.natureprotocols.com/2009/09/03/a\\_method\\_to\\_target\\_bioactive\\_c.php](http://www.natureprotocols.com/2009/09/03/a_method_to_target_bioactive_c.php). All mice were double-gavaged twice a week for five consecutive weeks (weeks 4–8) with or without encapsulated scCD98-functionalized NPs. Mice receiving siRNA-loaded NPs were treated with 1 mg/kg of siCD98 or scrambled siRNA (Life Technologies) each time.

### Induction of Acute Colitis and Oral siRNA Delivery

Acute colitis was induced in male C57BL/6 mice (10–12-wk-old) by replacing their drinking water with a 3.5% (wt/vol) DSS (36–50 kDa, MP Biomedicals). For each of the animal experiments, groups of mice were treated with DSS or normal water for six days. Mice were observed daily and evaluated for changes in body weight and development of clinical symptoms of colitis. Starting on day two, all the mice were double-gavaged daily for 4 consecutive days (that is, days 2–5) with or without encapsulated scCD98-functionalized NPs (weight ratio, 40:20:1). Mice receiving siRNA-loaded NPs were treated with 2 mg/kg of siCD98 or scrambled siRNA per day.

### In Vivo Gene Silencing Efficiency by qRT-PCR

Total RNA was extracted from the tissue samples using RNeasy Plus Mini Kit (Qiagen). The cDNA was generated from the total RNAs isolated above using the Maxima first strand cDNA synthesis kit (Fermentas) according to the manufacturer's instruction. Levels of CD98 RNA expression were quantified by real-time RT-PCR using Maxima® SYBR Green/ROX qPCR Master Mix (Fermentas).

## Histological Analysis of Tissue Sections by H&E Staining

Tissue samples were evaluated for mucosal architecture change, cellular infiltration, inflammation, goblet cell depletion, surface epithelial cell hyperplasia, and signs of epithelial regeneration using light microscopy of Haematoxylin and Eosin (H&E) staining. These values were used to assess the degrees of mucosal damage and repair in treatment and control groups. Tissues from RAG<sup>-/-</sup> mice were fixed in 10% buffered formalin (Fisher) and embedded in paraffin. And tissues from C57BL/6 were embedded in OCT. Tissue sections with a thickness of 6µm were stained with heomatoxylin and eosin followed by imaging using bright-field microscopy.

## Myeloperoxidase (MPO) Activity

Neutrophil infiltration into the colon was quantified by measuring MPO activity. Briefly, a portion of colon was homogenized in 1:20 (w/v) of 50 mM phosphate buffer (pH 6.0) containing 0.5% hexadecyltrimethyl ammonium bromide (Sigma) on ice using a homogenizer (Polytron, Luzern, Switzerland). The homogenate was then sonicated for 10s, freeze-thawed three times, and centrifuged at 16,000 g for 15 min. The supernatant (14 µL) was then added to 1 mg/mL *O*-dianisidine hydrochloride (Sigma) and 0.0005% hydrogen peroxide, and the change in absorbance at 460 nm was measured. MPO activity was expressed as units per mg of protein, where one unit was defined as the amount that degrades 1 µmol of hydrogen peroxide per min at 25 °C.

## Flow Cytometry Analysis

To investigate the ratio of each cells type in NPs uptake, the experiments were carried out in C57BL/6 mouse (12 week). Colitis was induced by replacing their drinking water with a 3.5% (wt/vol) DSS (36–50 kDa). To deliver the scCD98-functionalized FITC-siRNA-loaded NPs to mice colonic lumen, we encapsulated them into a hydrogel comprised of alginate and chitosan at a ratio of 7/3 (wt/wt) and double-gavaged the mice with or without treatment at day 5 of DSS treatment. After 12 h, the mice were humanly euthanized. Then spleen and colon were removed. Isolation of splenocytes and lamina propria immune cells was conducted as previously described [4, 5]. For splenocytes, spleens were dissected and cut into small fragments. The tissue was deposited on the nylon mesh and squeezed by the syringe handle. The tissue residues were rinsed using Hank's Buffered Salt Solution (HBSS, Life Technologies) with 5% FBS. The cells were collected by centrifugation at 300 rpm for 10 min. For cells from the colon tissue, colons were removed and carefully cleaned of their mesentery, and then the intestines were opened longitudinally and washed of fecal contents. Intestines were then cut into pieces 0.5 cm in length, which were transferred into 50 mL conical tubes and shaken at 220 rpm for 20 min at 37 °C in HBSS with 5% FBS containing 2 mM EDTA. This process was repeated two additional times. Cells suspensions were passed through a strainer and the remaining intestinal tissue was washed and then minced, transferred to a 50 mL conical tube and shaken for 20 min at 37 °C in HBSS with 5% FBS and type VIII collagenase (1.5 mg/mL; Sigma). Cell suspensions were collected and passed through a strainer and were pelleted by centrifugation at 300 rpm for 10 min.

Isolated splenocytes or colon cells were resuspended in PBS containing 5% FBS. After incubation for 15 min at 4 °C with the blocking Ab 2.4G2 anti-FcγRIII/I (eBioscience), the

cells were stained at 4 °C for 30 min with labeled Abs. Samples then were washed twice in PBS containing 5% FBS. The samples were analyzed immediately at this point, or they were fixed in PBS containing 2% paraformaldehyde and stored at 4 °C. Antibodies used for analysis were from eBioscience unless otherwise noted: anti-mouse CD98 Alexa Fluor 647 (Biolegend), anti-Mouse CD11c APC, anti-mouse CD11b eFluor<sup>®</sup> 450, anti-mouse F4/80 antigen PE-Cy7, anti-mouse CD4 Alexa Fluor 647 (Biolegend), anti-mouse CD4 APC, anti-mouse CD4 eFluor<sup>®</sup> 450, anti-mouse CD4 PE-Cy7 and anti-mouse CD4 FITC (BD pharmingen). Flow cytometric analysis was performed on a BD LSRFortessa flow cytometer (BD Biosciences) and data was analyzed using the FlowJo v10 processing program.

### Statistical Analysis

Statistical analysis was performed using a two-tailed unpaired Student's *t*-test. Data were expressed as mean ± standard error of mean (S.E.M.). Statistical significance was represented by \**P*<0.05 and \*\**P*<0.01.

### Supplementary Material

Refer to Web version on PubMed Central for supplementary material.

### Abbreviations used in this paper

<b>APC</b>	allophycocyanin
<b>BMDM</b>	bone marrow-derived macrophage
<b>BSA</b>	bovine serum albumin
<b>DAPI</b>	4',6-diamidino-2-phenyl-indole dihydrochloride
<b>DSS</b>	dextran sodium sulfate
<b>ECIS</b>	electrical impedance sensing
<b>FBS</b>	fetal bovine serum
<b>FCM</b>	flow cytometry
<b>H&amp;E</b>	hematoxylin and eosin
<b>IBD</b>	inflammatory bowel disease
<b>LPS</b>	lipopolysaccharide
<b>MPO</b>	myeloperoxidase
<b>MTT</b>	3-(4,5-dimethylthiazol-2-yl)-2,5-diphenyl tetrazolium bromide assay
<b>NP</b>	nanoparticle
<b>PBS</b>	phosphate-buffered saline
<b>PE</b>	phycoerythrin



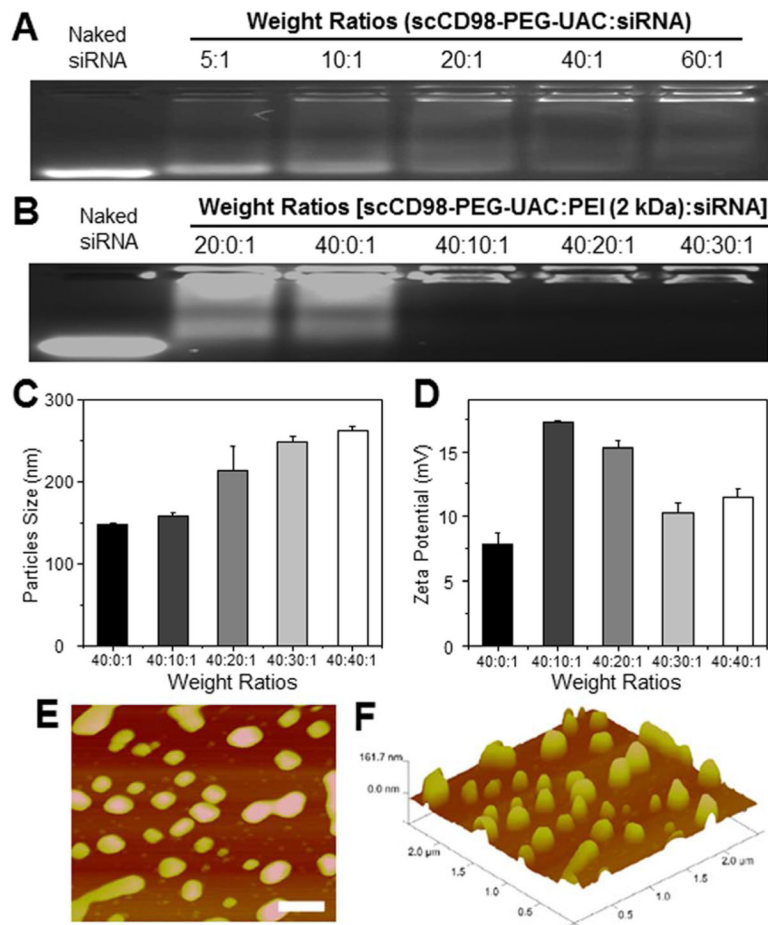
<b>PEG</b>	poly(ethylene glycol)
<b>PEI</b>	polyethylenimine
<b>RAG<sup>-/-</sup> mice</b>	recombinase activating gene-1-deficient mice
<b>RNAi</b>	RNA interference
<b>scCD98</b>	single-chain CD98 antibody
<b>scCD98-PEG-UAC</b>	single-chain CD98 antibody-poly(ethylene glycol)-urocanic acid-modified chitosan
<b>siCD98</b>	CD98 siRNA
<b>siRNA</b>	small interfering RNA
<b>SPR</b>	surface plasmon resonance
<b>qRT-PCR</b>	quantitative reverse-transcription polymerase chain reaction

## References

1. Nguyen HT, Dalmaso G, Torkvist L, et al. CD98 expression modulates intestinal homeostasis, inflammation, and colitis-associated cancer in mice. *J Clin Invest*. 2011; 121:1733–1747. [PubMed: 21490400]
2. Pineton de Chambrun G, Peyrin-Biroulet L, Lemann M, et al. Clinical implications of mucosal healing for the management of IBD. *Nat Rev Gastroenterol Hepatol*. 2010; 7:15–29. [PubMed: 19949430]
3. Iacucci M, de Silva S, Ghosh S. Mesalazine in inflammatory bowel disease: a trendy topic once again? *Can J Gastroenterol*. 2010; 24:127–133. [PubMed: 20151072]
4. Xiao B, Merlin D. Oral colon-specific therapeutic approaches toward treatment of inflammatory bowel disease. *Expert Opin Drug Deliv*. 2012; 9:1393–1407. [PubMed: 23036075]
5. Yan Y, Vasudevan S, Nguyen HT, et al. Intestinal epithelial CD98: an oligomeric and multifunctional protein. *Biochim Biophys Acta*. 2008; 1780:1087–1092. [PubMed: 18625289]
6. Nguyen HT, Merlin D. Homeostatic and innate immune responses: role of the transmembrane glycoprotein CD98. *Cell Mol Life Sci*. 2012; 69:3015–3026. [PubMed: 22460579]
7. Kucharzik T, Luger A, Yan Y, et al. Activation of epithelial CD98 glycoprotein perpetuates colonic inflammation. *Lab Invest*. 2005; 85:932–941. [PubMed: 15880135]
8. Nguyen HT, Dalmaso G, Yan Y, et al. MicroRNA-7 modulates CD98 expression during intestinal epithelial cell differentiation. *J Biol Chem*. 2010; 285:1479–1489. [PubMed: 19892711]
9. Schreiber S, MacDermott RP, Raedler A, et al. Increased activation of isolated intestinal lamina propria mononuclear cells in inflammatory bowel disease. *Gastroenterology*. 1991; 101:1020–1030. [PubMed: 1889695]
10. MacKinnon AC, Farnworth SL, Hodgkinson PS, et al. Regulation of alternative macrophage activation by galectin-3. *J Immunol*. 2008; 180:2650–2658. [PubMed: 18250477]
11. Charania MA, Laroui H, Liu H, et al. Intestinal epithelial CD98 directly modulates the innate host response to enteric bacterial pathogens. *Infect Immun*. 2013; 81:923–934. [PubMed: 23297381]
12. Muza-Moons MM, Koutsouris A, Hecht G. Disruption of cell polarity by enteropathogenic *Escherichia coli* enables basolateral membrane proteins to migrate apically and to potentiate physiological consequences. *Infect Immun*. 2003; 71:7069–7078. [PubMed: 14638797]
13. Medarova Z, Pham W, Farrar C, et al. In vivo imaging of siRNA delivery and silencing in tumors. *Nat Med*. 2007; 13:372–377. [PubMed: 17322898]

14. Malmö J, Sorgard H, Varum KM, et al. siRNA delivery with chitosan nanoparticles: Molecular properties favoring efficient gene silencing. *J Control Release*. 2012; 158:261–268. [PubMed: 22119955]
15. Ganta S, Devalapally H, Shahiwala A, et al. A review of stimuli-responsive nanocarriers for drug and gene delivery. *J Control Release*. 2008; 126:187–204. [PubMed: 18261822]
16. Xiao B, Laroui H, Ayyadurai S, et al. Mannosylated bioreducible nanoparticle-mediated macrophage-specific TNF-alpha RNA interference for IBD therapy. *Biomaterials*. 2013; 34:7471–7482. [PubMed: 23820013]
17. Wang YY, Lai SK, Suk JS, et al. Addressing the PEG mucoadhesivity paradox to engineer nanoparticles that “slip” through the human mucus barrier. *Angew Chem Int Ed Engl*. 2008; 47:9726–9729. [PubMed: 18979480]
18. Kim TH, Ihm JE, Choi YJ, et al. Efficient gene delivery by urocanic acid-modified chitosan. *J Control Release*. 2003; 93:389–402. [PubMed: 14644588]
19. Liu Y, Reineke TM. Hydroxyl stereochemistry and amine number within poly(glycoamidoamine)s affect intracellular DNA delivery. *J Am Chem Soc*. 2005; 127:3004–3015. [PubMed: 15740138]
20. Ryser HJ. A membrane effect of basic polymers dependent on molecular size. *Nature*. 1967; 215:934–936. [PubMed: 6055419]
21. Felgner JH, Kumar R, Sridhar CN, et al. Enhanced gene delivery and mechanism studies with a novel series of cationic lipid formulations. *J Biol Chem*. 1994; 269:2550–2561. [PubMed: 8300583]
22. Bottega R, Epanand RM. Inhibition of protein kinase C by cationic amphiphiles. *Biochemistry*. 1992; 31:9025–9030. [PubMed: 1390689]
23. Marim FM, Silveira TN, Lima DS Jr, et al. A method for generation of bone marrow-derived macrophages from cryopreserved mouse bone marrow cells. *PLoS One*. 2010; 5:e15263. [PubMed: 21179419]
24. Munitz A, Cole ET, Beichler A, et al. Paired immunoglobulin-like receptor B (PIR-B) negatively regulates macrophage activation in experimental colitis. *Gastroenterology*. 2010; 139:530–541. [PubMed: 20398663]
25. Schneider F, Sukhova GK, Aikawa M, et al. Matrix-metalloproteinase-14 deficiency in bone-marrow-derived cells promotes collagen accumulation in mouse atherosclerotic plaques. *Circulation*. 2008; 117:931–939. [PubMed: 18250269]
26. Ostanin DV, Bao J, Koboziev I, et al. T cell transfer model of chronic colitis: concepts, considerations, and tricks of the trade. *Am J Physiol Gastrointest Liver Physiol*. 2009; 296:G135–146. [PubMed: 19033538]
27. Grisham MB. Do different animal models of IBD serve different purposes? *Inflamm Bowel Dis*. 2008; 14 (Suppl 2):S132–133. [PubMed: 18816751]
28. Perse M, Cerar A. Dextran sodium sulphate colitis mouse model: traps and tricks. *J Biomed Biotechnol*. 2012; 2012:718617. [PubMed: 22665990]
29. Zhu Q, Talton J, Zhang G, et al. Large intestine-targeted, nanoparticle-releasing oral vaccine to control genitorectal viral infection. *Nat Med*. 2012; 18:1291–1296. [PubMed: 22797811]
30. Veettil MV, Sadagopan S, Sharma-Walia N, et al. Kaposi’s sarcoma-associated herpesvirus forms a multimolecular complex of integrins (alphaVbeta5, alphaVbeta3, and alpha3beta1) and CD98-xCT during infection of human dermal microvascular endothelial cells, and CD98-xCT is essential for the postentry stage of infection. *J Virol*. 2008; 82:12126–12144. [PubMed: 18829766]
31. Ohkame H, Masuda H, Ishii Y, et al. Expression of L-type amino acid transporter 1 (LAT1) and 4F2 heavy chain (4F2hc) in liver tumor lesions of rat models. *J Surg Oncol*. 2001; 78:265–271. [PubMed: 11745822]
32. Cantor JM, Ginsberg MH. CD98 at the crossroads of adaptive immunity and cancer. *J Cell Sci*. 2012; 125:1373–1382. [PubMed: 22499670]
33. Khalil IA, Kogure K, Akita H, et al. Uptake pathways and subsequent intracellular trafficking in nonviral gene delivery. *Pharmacol Rev*. 2006; 58:32–45. [PubMed: 16507881]
34. Laroui H, Dalmaso G, Nguyen HT, et al. Drug-loaded nanoparticles targeted to the colon with polysaccharide hydrogel reduce colitis in a mouse model. *Gastroenterology*. 2010; 138:843–53. e1–2. [PubMed: 19909746]

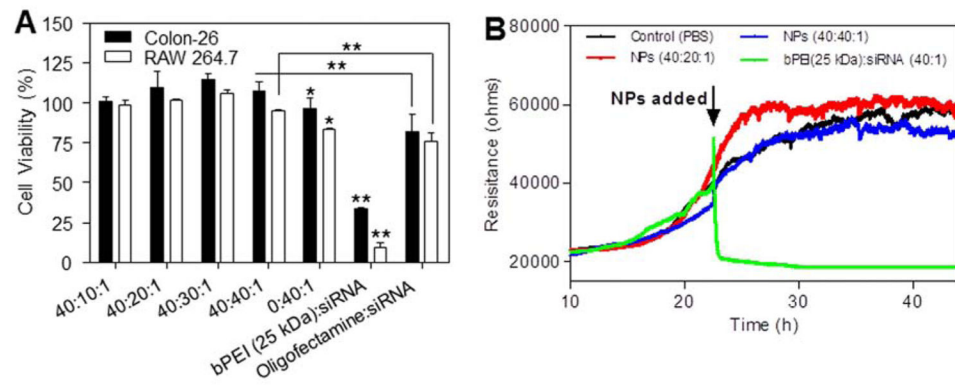
35. Laroui H, Theiss AL, Yan Y, et al. Functional TNF $\alpha$  gene silencing mediated by polyethyleneimine/TNF $\alpha$  siRNA nanocomplexes in inflamed colon. *Biomaterials*. 2011; 32:1218–1228. [PubMed: 20970849]
36. Theiss AL, Laroui H, Obertone TS, et al. Nanoparticle-based therapeutic delivery of prohibitin to the colonic epithelial cells ameliorates acute murine colitis. *Inflamm Bowel Dis*. 2011; 17:1163–1176. [PubMed: 20872832]
1. Kim TH, Ihm JE, Choi YJ, et al. Efficient gene delivery by urocanic acid-modified chitosan. *J Control Release*. 2003; 93:389–402. [PubMed: 14644588]
2. Ostanin DV, Kurmaeva E, Furr K, et al. Acquisition of antigen-presenting functions by neutrophils isolated from mice with chronic colitis. *J Immunol*. 2012; 188:1491–1502. [PubMed: 22219329]
3. Ostanin DV, Bao J, Koboziev I, et al. T cell transfer model of chronic colitis: concepts, considerations, and tricks of the trade. *Am J Physiol Gastrointest Liver Physiol*. 2009; 296:G135–146. [PubMed: 19033538]
4. Denning TL, Wang YC, Patel SR, et al. Lamina propria macrophages and dendritic cells differentially induce regulatory and interleukin 17-producing T cell responses. *Nat Immunol*. 2007; 8:1086–1094. [PubMed: 17873879]
5. Denning TL, Norris BA, Medina-Contreras O, et al. Functional specializations of intestinal dendritic cell and macrophage subsets that control Th17 and regulatory T cell responses are dependent on the T cell/APC ratio, source of mouse strain, and regional localization. *J Immunol*. 2011; 187:733–747. [PubMed: 21666057]



**Figure 1.**

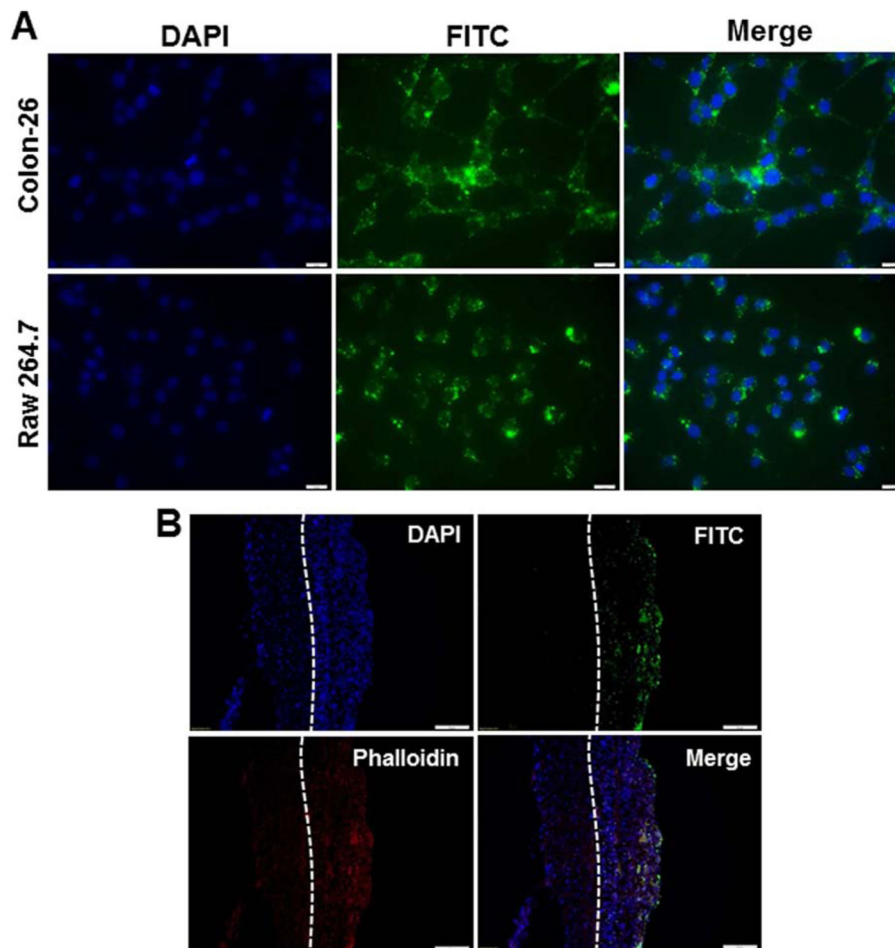
Physicochemical and morphological characterization of scCD98-functionalized NPs.

Agarose gel electrophoresis of NPs with different weight ratios: (A) scCD98-functionalized NPs prepared by scCD98-PEG-UAC and scrambled siRNA; (B) scCD98-functionalized NPs fabricated by scCD98-PEG-UAC and scrambled siRNA with different amounts of PEI (2 kDa). Particle sizes (C) and zeta potential (D) of scCD98-functionalized NPs with different weight ratios measured by dynamic light scattering. Each point represents the mean  $\pm$  S.E.M. ( $n = 3$ ). The height scanning profile (E) and topographical data (F) of atomic force micrograph show scCD98-functionalized NPs (weight ratio, 40:20:1). Scale bar represents 500 nm.

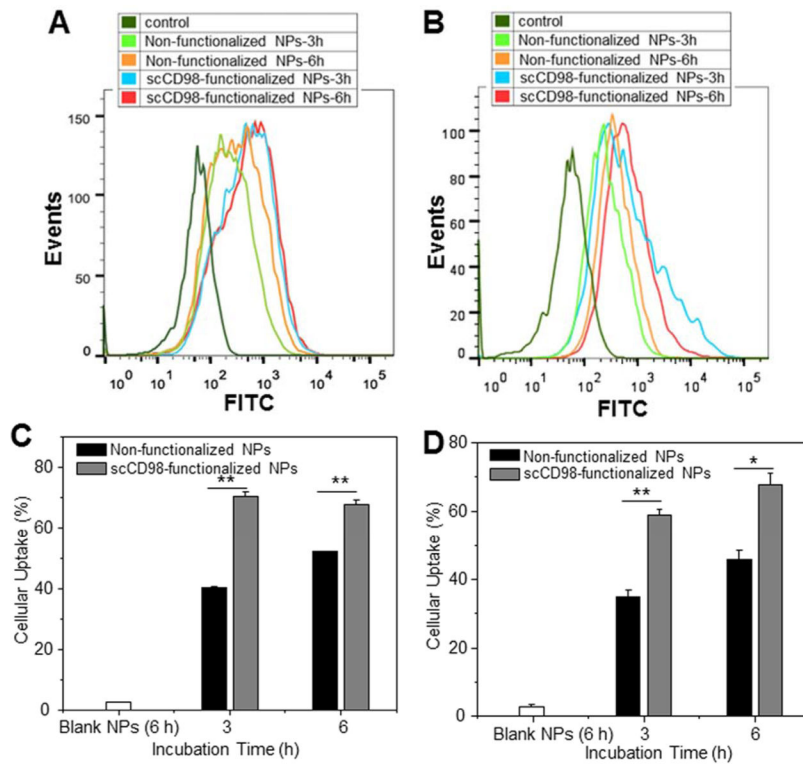


**Figure 2.**

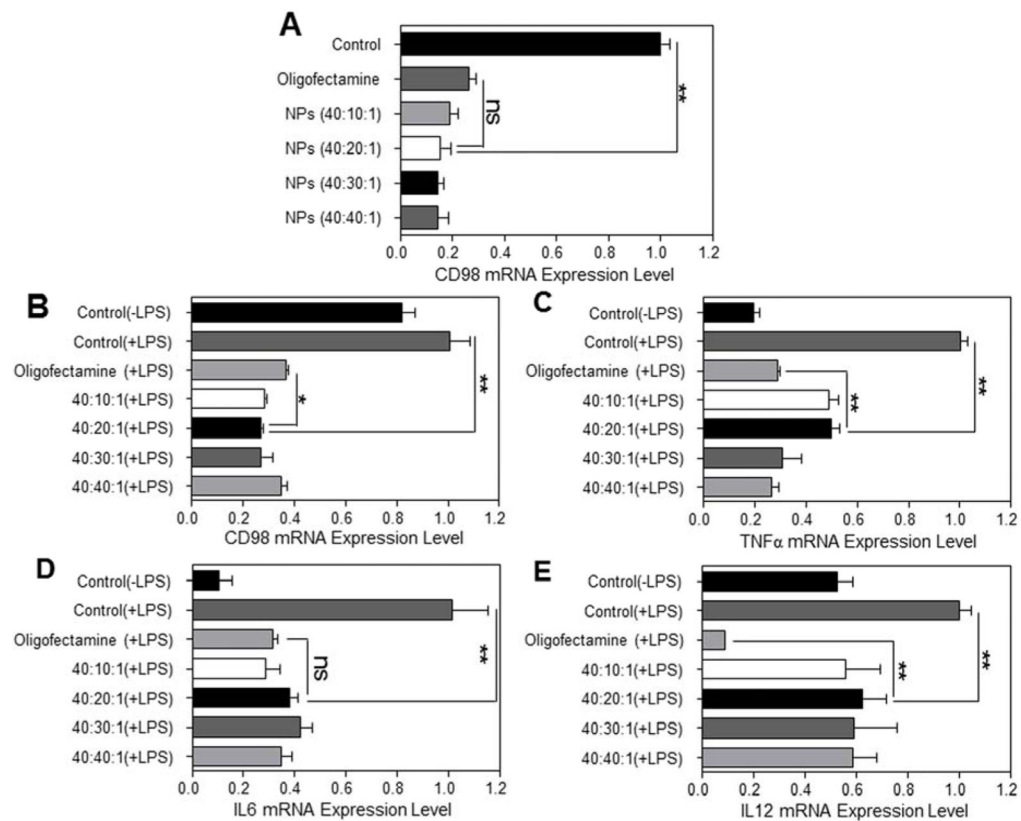
Cytotoxicity test of scCD98-functionalized NPs against Colon-26 cells, RAW 267.4 macrophages and Caco2-BBE cells. (A) The MTT tests were used to determine the cytotoxicities of scCD98-functionalized NPs, and compared to PEI (2 kDa)/siRNA complexes, bPEI (25 kDa)/siRNA complexes and Oligofectamine/siRNA complexes. For experiments, siRNA was used at a concentration of 100 nM except for the Oligofectamine/siRNA complexes, which were generated according to the manufacturer's standard protocols. Toxicity is given as the percentage of viable cells remaining after treatment for 6 h. Each point represents the mean  $\pm$  S.E.M. (n=5). Statistical significance was assessed using the Student's *t*-test (\* $P$ <0.05 and \*\* $P$ <0.01). (B) Electrical impedance-sensing (ECIS) of Caco2-BBE cells was used to determine cell viability after a long exposure to a NPs suspensions. As controls, ECIS was also performed on untreated cells and cells treated with bPEI (25 kDa)/siRNA complexes. The siRNA concentration in the medium is set as 100 nM (n=2).



**Figure 3.** Uptake profiles of scCD98-functionalized FITC-siRNA-loaded NPs (weight ratio, 40:20:1) by Colon-26 cells, RAW 267.4 macrophages and colitis tissue. (A) Cellular uptake of NPs by respective Colon-26 cells and RAW 267.4 cells. Cells were treated with NPs (green) and processed for fluorescence staining. FITC-siRNA with the concentration of 100 nM was used for the transfections. Fixed cells were stained with DAPI for visualization of nuclei (purple). Scale bar represents 10  $\mu$ m. (B) Colitis tissue uptake of NPs after 6 h of co-incubation. Colitis tissues were treated with NPs (green), sectioned and processed for fluorescence staining. FITC-siRNA with the concentration of 200 nM was used for the transfections. Fixed tissues were stained with Alexa Fluor 568 phalloidin and DAPI to visualize actin (red) and nuclei (purple), respectively (n=3). Scale bar represents 50  $\mu$ m.



**Figure 4.** Quantification of cellular uptake of FITC-siRNA-loaded NPs (weight ratio, 40:20:1) by Colon-26 and RAW 264.7 cells at different time points (3 h and 6 h). Flow cytometry histogram overlays show the cellular uptake of NPs by Colon-26 cells (A) and RAW 267.4 macrophages (B). Analysis of the percentage of FITC fluorescence-positive Colon-26 cells (C) and RAW 267.4 macrophages (D). FITC-siRNA with the concentration of 100 nM was used for the transfections. Each point represents the mean  $\pm$  S.E.M. (n=3). Statistical significance was assessed using the Student's *t*-test (\* $P$ <0.05 and \*\* $P$ <0.01).

**Figure 5.**

*In vitro* RNAi ability of scCD98-functionalized siCD98-loaded NPs against Colon-26 and RAW 267.4 macrophages. (A) CD98 mRNA expression levels of Colon-26 cells exposed to NPs. Cells were transfected by NPs (siRNA, 100 nM) for 24 h. The mRNA expression levels of CD98 (B) and the pro-inflammatory cytokines, namely TNF $\alpha$  (C), IL6 (D) and IL12(E) for RAW 264.7 macrophages exposed to NPs. Cells were transfected by NPs (siRNA, 100 nM) for 24 h, and then treated with LPS (5  $\mu$ g/mL) for 3 h. Oligofectamine was used according to the manufacturer's standard protocols. Each point represents the mean  $\pm$  S.E.M. (n=3). Statistical significance was assessed using the Student's *t*-test (\* $P$ <0.05, \*\* $P$ <0.01; ns, non-significant).



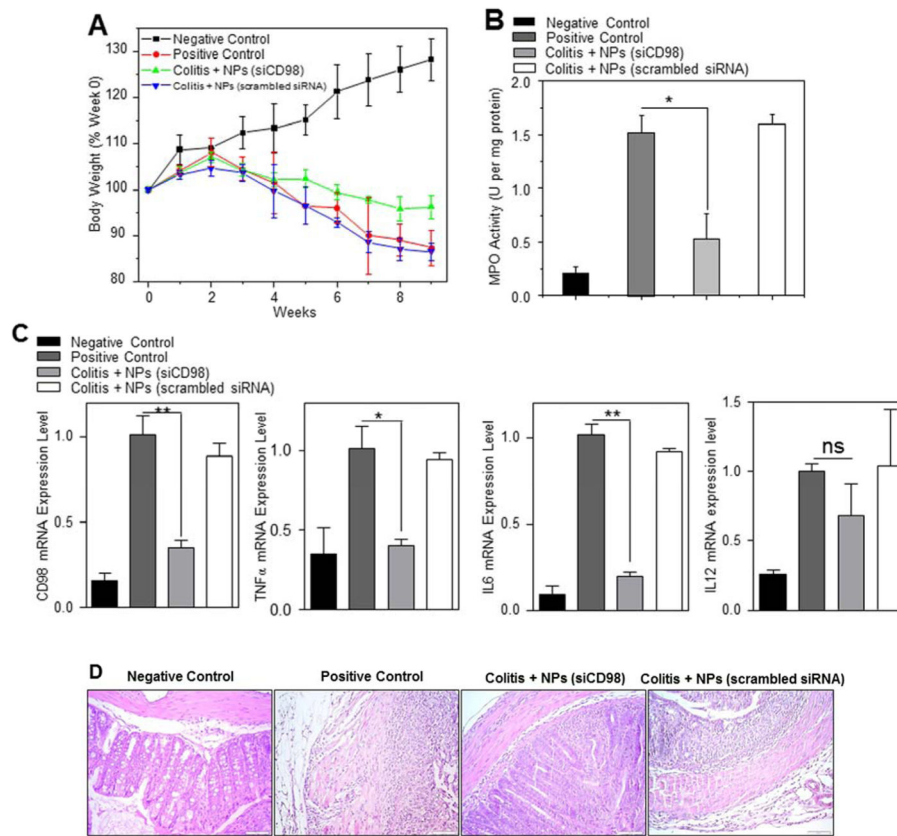


**Figure 6.**

Oral administration of scCD98-functionalized siCD98-loaded NPs decreases chronic colitis in RAG<sup>-/-</sup> mice. (A) Mouse body weight over time, normalized as a percentage of week zero body weight and given as the mean of each treatment group. (B) Colonic myeloperoxidase (MPO) activity. The results are expressed as units of MPO activity per milligram of protein. (C) The mRNA levels of CD98 and pro-inflammatory cytokines in mice with different treatments. (D) Representative H&E-stained colon sections from mice administered with hydrogel in the present or absent of NPs for 5 weeks. Scale bar represents 50  $\mu$ m. Each point represents the mean  $\pm$  S.E.M. (n=4). Statistical significance was assessed using the Student's *t*-test (\* $P$ <0.05, \*\* $P$ <0.01; ns, non-significant).

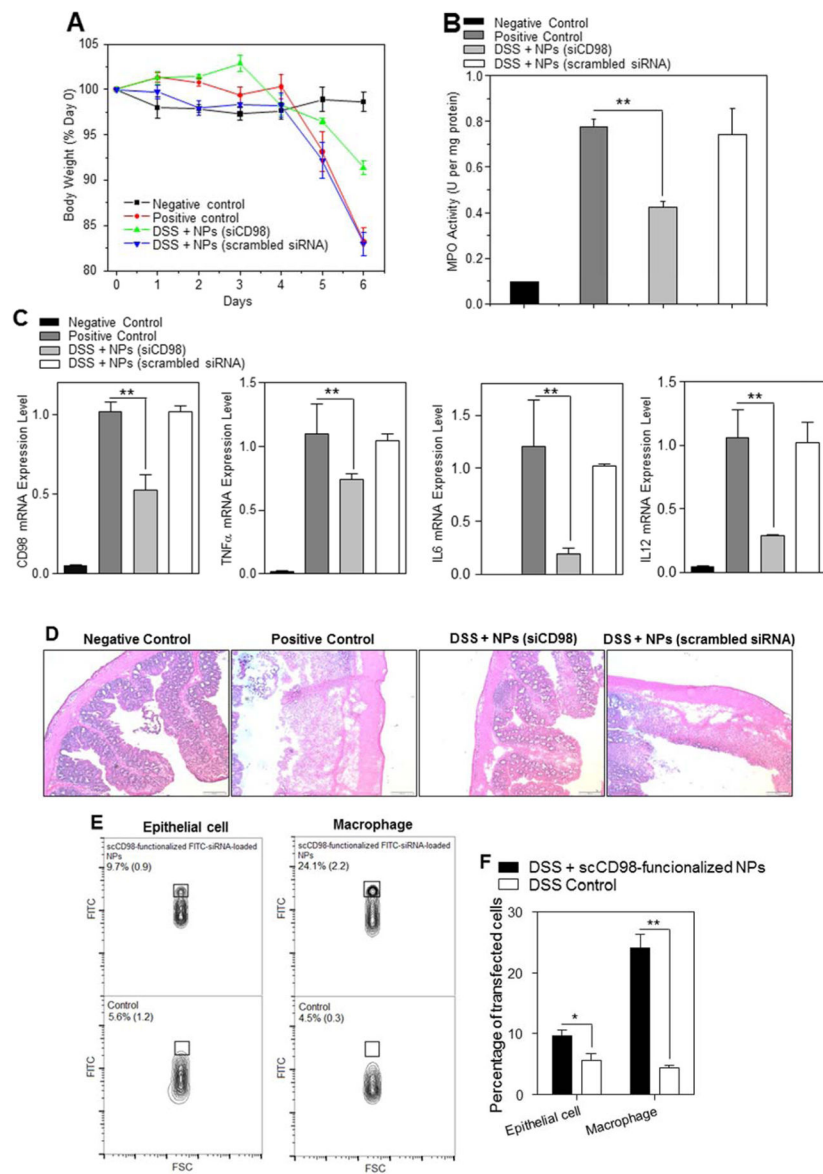


**Figure 7.**

Oral administration of scCD98-functionalized siCD98-loaded NPs decrease acute colitis induced by DSS. (A) Mouse body weight over time, normalized as a percentage of day zero body weight and given as the mean of each treatment group. (B) Colonic myeloperoxidase (MPO) activity. The results are expressed as units of MPO activity per milligram of protein. (C) The mRNA levels of CD98 and pro-inflammatory cytokines in mice with different treatments. Each point represents the mean  $\pm$  S.E.M. (n=5). Statistical significance was assessed using the Student's *t*-test (\* $P$ <0.05 and \*\* $P$ <0.01). (D) Representative H&E-stained colon sections from DSS-treated mice administered with daily double gavages of hydrogel with or without NPs for 4 days. Scale bar represents 100  $\mu$ m. (E) Representative FCM analysis and (F) percentage of FITC fluorescence-positive colon epithelial cells and macrophages in mice receiving DSS and treated with hydrogel with or without scCD98-

functionalized FITC-siRNA-loaded NPs. Data are expressed as mean  $\pm$  S.E.M. (n=3). Statistical significance was performed using Student's *t*-test (\* $P$ <0.05 and \*\* $P$ <0.01).